JACS
JOURNAL OF THE AMERICAN CHEMICAL SOCIETY
pubs.acs.org/JACS
Article

Ligand-Regulated Metallaphotoredox Aminoarylation for the Valorization of Feedstock Alkenes

Weigang Zhang, Zhexuan Lei, Tao Liu, Xiao Guo, Jiahe Shen, Jianke Su, Yan Li, Jiale Wu, Hong Jiang, Hwee Ting Ang, Yixin Luo,* Xingwei Guo, Yu Lan,* and Jie Wu*

Cite This: https://doi.org/10.1021/jacs.6c03412
Read Online
ACCESS | Metrics & More | Article Recommendations | Supporting Information

ABSTRACT: N-(Hetero)aryl-substituted arylethylamine derivatives are privileged scaffolds with broad biological activity for drug discovery. However, current synthetic approaches are limited by reliance on prefunctionalized substrates, multistep protocols, and harsh conditions. Free N−H bonds in amines can deactivate transition-metal catalysts through coordination. To overcome these limitations, we herein report a practical ligand-regulated metallaphotoredox-catalyzed aminoarylation of ethylene for the direct access to diverse N-(hetero)aryl-substituted arylethylamines from readily available feedstocks, including arenes and (hetero)arylamines. Key to this transformation is the use of diaryl-substituted 1,3-diketone ligands, which effectively modulate the reactivity of the single-electron transfer and proton transfer steps. Our approach not only streamlines the synthesis of structurally diverse N-(hetero)aryl-substituted arylethylamines with excellent functional group tolerance, but also provides a new paradigm for converting ethylene into complex, pharmaceutical relevant molecules. Moreover, the protocol is applicable to propylene, nongaseous alkenes, and 1,3-dienes, underscoring its broad utility in transforming abundant petrochemical feedstocks into value-added products.

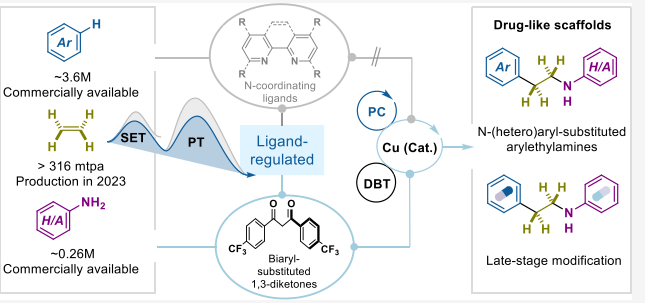

INTRODUCTION

β-(Hetero)arylethylamines are prevalent in pharmaceuticals due to their extensive array of biological activities, making them a privileged scaffold in drug discovery.[1−4] Among these, the N-(hetero)aryl-substituted arylethylamine scaffold has emerged as a particularly promising structural motif. A remarkable catalog of over 57,000 compounds of this type has been recorded, with approximately 39% demonstrating relevance in various bioactivity studies (Figure 1A). Notable examples include *crisdesalazine* (also known as AAD-2004), developed for the treatment of Alzheimer's disease, Parkinson's disease, and amyotrophic lateral sclerosis (ALS);[5] *fanetizole*, an immunomodulatory agent;[6] and *flufenerim*,[7] a diarylethylamine-based agrochemical with potent activity against the sweet potato whitefly and the green peach aphid.

Conventionally, N-(hetero)aryl-substituted arylethylamines have been synthesized via the nucleophilic substitution of arylethyl halides with unprotected (hetero)arylamines,[8,9] a process that frequently affords undesired over alkylated byproducts. Transition-metal-catalyzed strategies have also been developed, including redox-neutral or oxidative cross-coupling of preformed arylethylamines with aryl electrophiles or nucleophiles such as aryl halides, diaryliodonium salts or arylboronic acids, which typically require elevated temperatures.[10−15] Hydroamination of styrenes with arylamines, under either transition-metal catalysis or metal-free conditions, provides another route to N-aryl-substituted arylethylamines, albeit typically requiring strongly basic conditions or high temperatures.[16−19] In addition, hydroamination of arylalkynes has been employed to access these motifs using hydrogen as the reductant.[20] Alternatively, condensation of phenylacetic acid or phenylacetaldehyde derivatives with primary arylamines, followed by hydrogenation, has been employed to access diarylethylamine frameworks.[21,22] Despite these advancements, current methodologies are often constrained by the need for prefunctionalized substrates (such as *β*-haloarylethane and arylacetic acid derivatives),[9,22] limited modularity,[9,22] lengthy synthetic sequences, and harsh reaction conditions.[17−20] There is, therefore, a compelling need for innovative and modular strategies that enable the direct construction of N-(hetero)aryl-substituted arylethylamines from readily available feedstocks, thereby broadening their accessibility for pharmaceutical development.

We propose that a modular three-component assembly involving ethylene, unprotected (hetero)arylamines, and

Received: February 13, 2026
Revised: May 4, 2026
Accepted: June 8, 2026

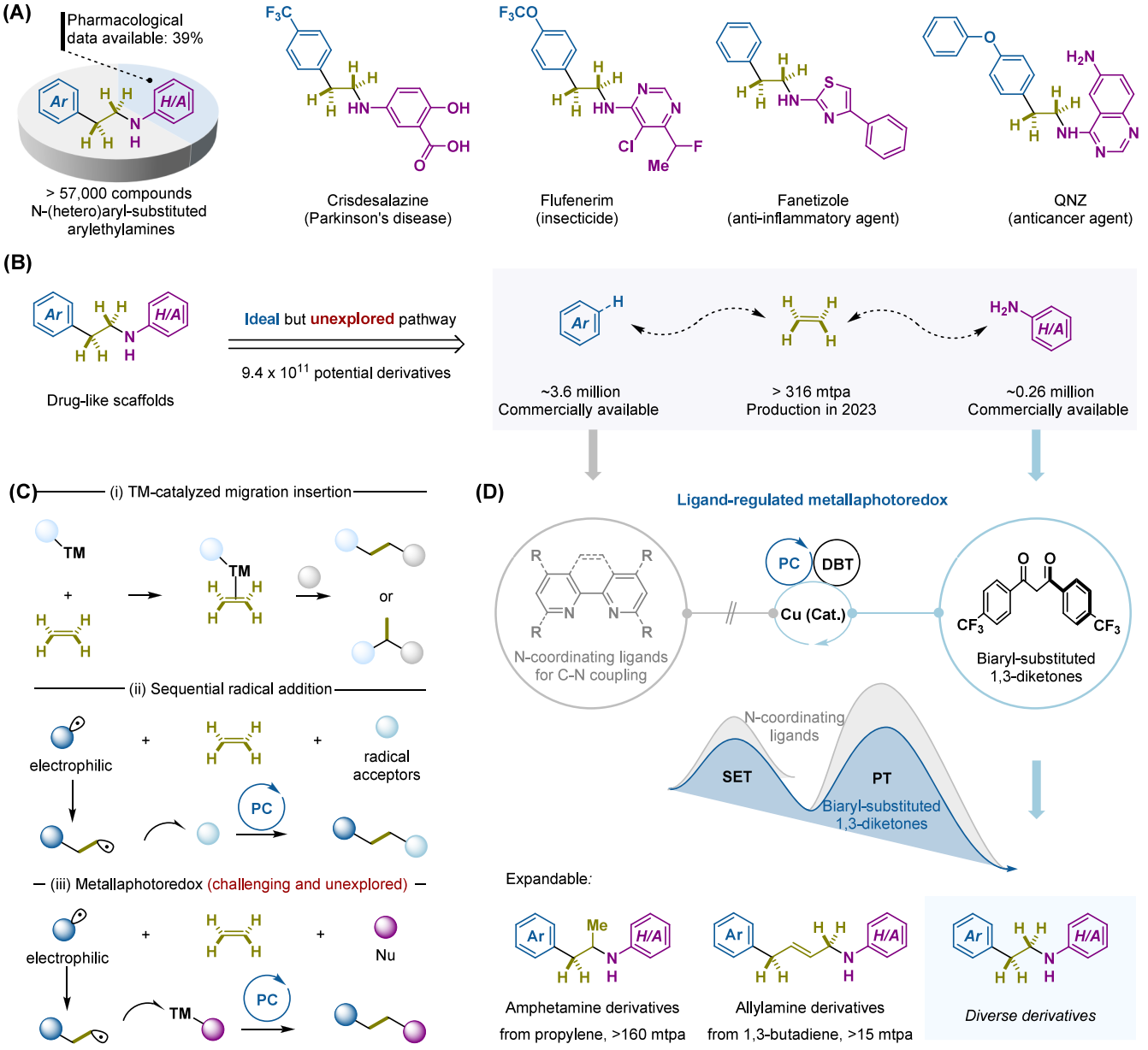

Figure 1. Strategies and challenges for the synthesis of N-(hetero)aryl-substituted arylethylamines through aminoarylation of ethylene. (A) Significance of N-(hetero)aryl-substituted arylethylamine scaffolds. A Reaxys search (April 2025) identified pharmacological data for 22,209 out of 57,116 reported N-(hetero)aryl-substituted arylethylamines. (B) Our working hypothesis for synthesizing N-(hetero)aryl arylethylamine derivatives. (C) Strategies for ethylene difunctionalization. (D) This study: modular approach for the synthesis of drug-like N-(hetero)aryl-substituted arylethylamines via ligand-regulated metallaphotoredox aminoarylation from abundant ethylene, arenes, and (hetero)arylamines. mtpa, million tonnes per annum; TM, transition metal; H/A, (hetero)aryl; DBT, dibenzothiophene; SET, single electron transfer; PT, proton transfer.

arenes would offer a practical and efficient strategy for accessing structurally diverse N-(hetero)aryl-substituted arylethylamine derivatives (Figure 1B). As the most abundant petrochemical product and a crucial C2 synthon, ethylene has garnered significant research interest in fine chemical synthesis,[23−28] with global production exceeding 316 million tons in 2023. Concurrently, readily available arenes, which are ubiquitous in natural products and pharmaceutically relevant molecules, can be readily activated through an air-stable and site-selective sulfonium salt formation, making them excellent precursors for aryl radical generation.[29−35] Despite notable advances in ethylene difunctionalization, the established synthetic strategies, such as transition-metal-catalyzed coupling via coordination and migratory insertion[23,36−41] or radical addition pathways[42−47] (Figure 1C, i and ii), are not applicable to three-component aminoarylation, likely due to the absence of appropriate catalytic systems. The metallaphotoredox strategy,[48] synergistically combining the exceptional bond-forming capacity of transition-metal catalysis with the versatility of photoinduced single-electron transfer (SET), has emerged as a transformative platform that opens new avenues for radical-based cross-couplings.

However, the metallaphotoredox-catalyzed aminoarylation of ethylene, with unprotected amines and arenes remains a formidable challenge and largely uncharted territory[49] (Figure 1C, iii) due to the inherently low rate of radical addition to ethylene compared to substituted alkenes,[50] the competing ethylene dimerization or oligomerization pathways under high-

https://doi.org/10.1021/jacs.6c03412
J. Am. Chem. Soc. XXXX, XXX, XXX−XXX

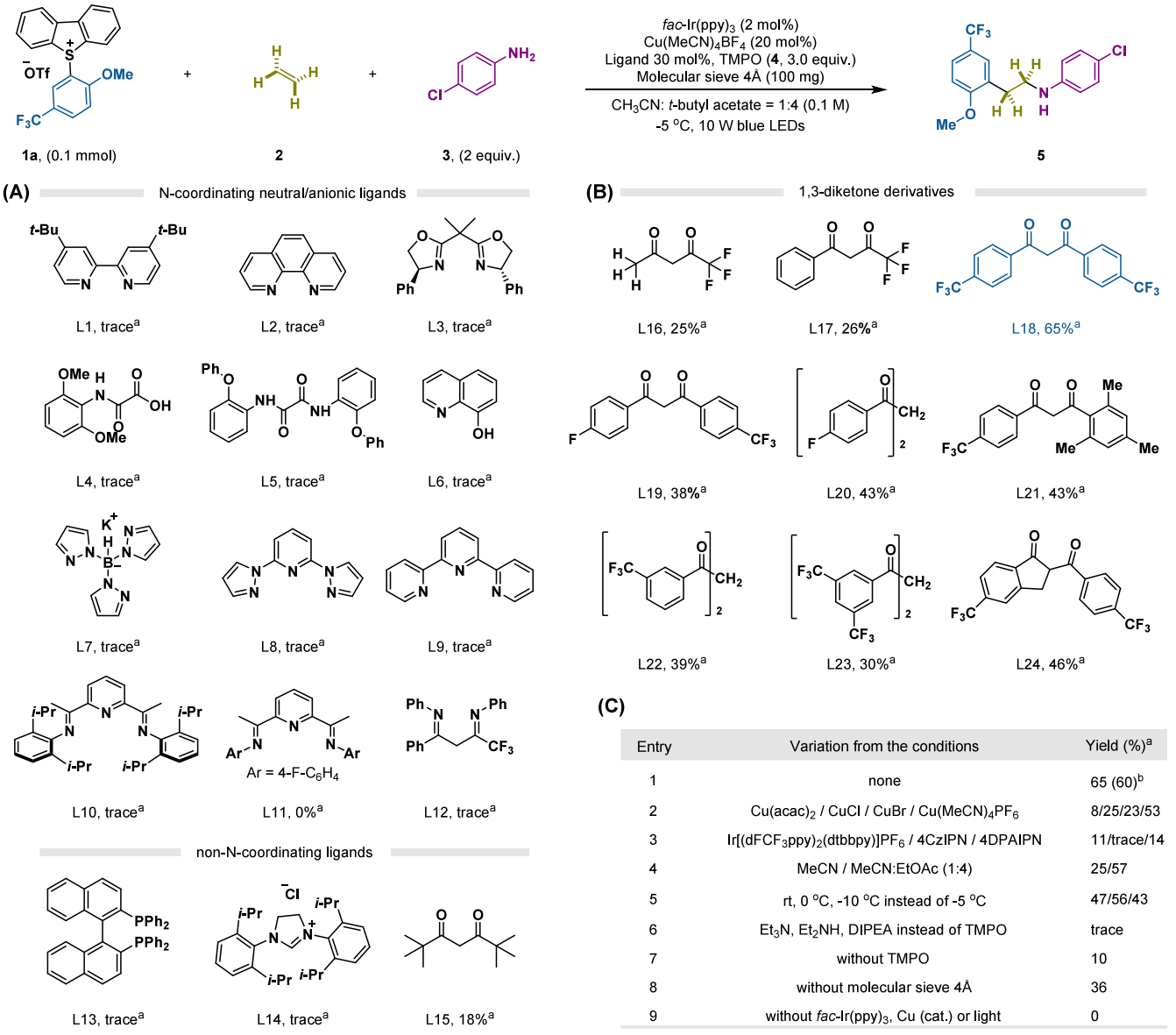

(C)

Entry	Variation from the conditions	Yield (%)[a]
1	none	65 (60)[b]
2	$Cu(acac)_2$ / CuCl / CuBr / $Cu(MeCN)_4PF_6$	8/25/23/53
3	$Ir[(dFCF_3ppy)_2(dtbbpy)]PF_6$ / 4CzIPN / 4DPAIPN	11/trace/14
4	MeCN / MeCN:EtOAc (1:4)	25/57
5	rt, 0 °C, -10 °C instead of -5 °C	47/56/43
6	Et_3N, Et_2NH, DIPEA instead of TMPO	trace
7	without TMPO	10
8	without molecular sieve 4Å	36
9	without *fac*-Ir(ppy)$_3$, Cu (cat.) or light	0

Figure 2. Exploration of reaction conditions. (A) Investigation of common neutral and anionic ligands. (B) Evaluation of various 1,3-diketone ligands. (C) Evaluation of other reaction parameters. [a]The yields were determined by analysis of the crude ^{1}H NMR spectra using CH_2Br_2 as an external standard. [b]Isolated yield in parentheses. DBT salt, aryl dibenzothiophenium salt; TMPO, 2,2,6,6-tetramethylpiperidin-4-one.

pressure conditions,[51] as well as the susceptibility of catalyst deactivation through coordination with Lewis basic amines.[52,53] Moreover, the primary alkyl radicals formed from the addition of aryl radicals to ethylene are only modestly stabilized (radical stabilization energy RSE ≈ −18.8 kJ·mol^{-1}),[54] which renders their controlled interception challenging and may complicate the subsequent reaction process. Additional complexity arises from competing pathways, including two-component C−N coupling, Heck-type reaction of aryl radicals with ethylene,[55] and Minisci-type addition of aryl radicals to heteroarylamines, all of which further hinder the desired three-component cross-coupling. Ligands are well recognized to play a pivotal role in transition-metal-catalyzed cross-coupling reactions by tuning the reactivity, selectivity, and stability of the metal center. Notably, although ligands such as phenanthrolines, bipyridines, bisoxazolines, as well as oxalate derivatives have demonstrated broad utility in C(sp^3)−N cross-coupling reactions,[56−58] they exhibit limited catalytic activity in the three-component aminoarylation of ethylene (for details, see Figure 2 and Tables S1 and S5−S6).

Herein, we disclosed a modular approach for the direct synthesis of N-(hetero)aryl-substituted arylethylamine derivatives through a ligand-regulated photoredox/copper catalyzed three-component carboamination of ethylene with commercially available feedstocks (Figure 1D). Key to the success of this transformation is the use of diaryl-substituted 1,3-diketones as ligands to promote the conversion of Cu(I) to Cu(II) intermediate through SET, while simultaneously enhancing the acidity of the hydrogen atoms in the coordinating arylamines to regulate the reactivity of the subsequent proton transfer (PT) process. The developed system showcases a broad substrate scope, accommodating a wide range of gaseous and nongaseous alkenes, arenes, and (hetero)arylamines, thus offering a versatile platform for the construction of diverse N-(hetero)aryl-substituted arylethylamines. Additionally, leveraging propylene and 1,3-butadiene

https://doi.org/10.1021/jacs.6c03412
J. Am. Chem. Soc. XXXX, XXX, XXX−XXX

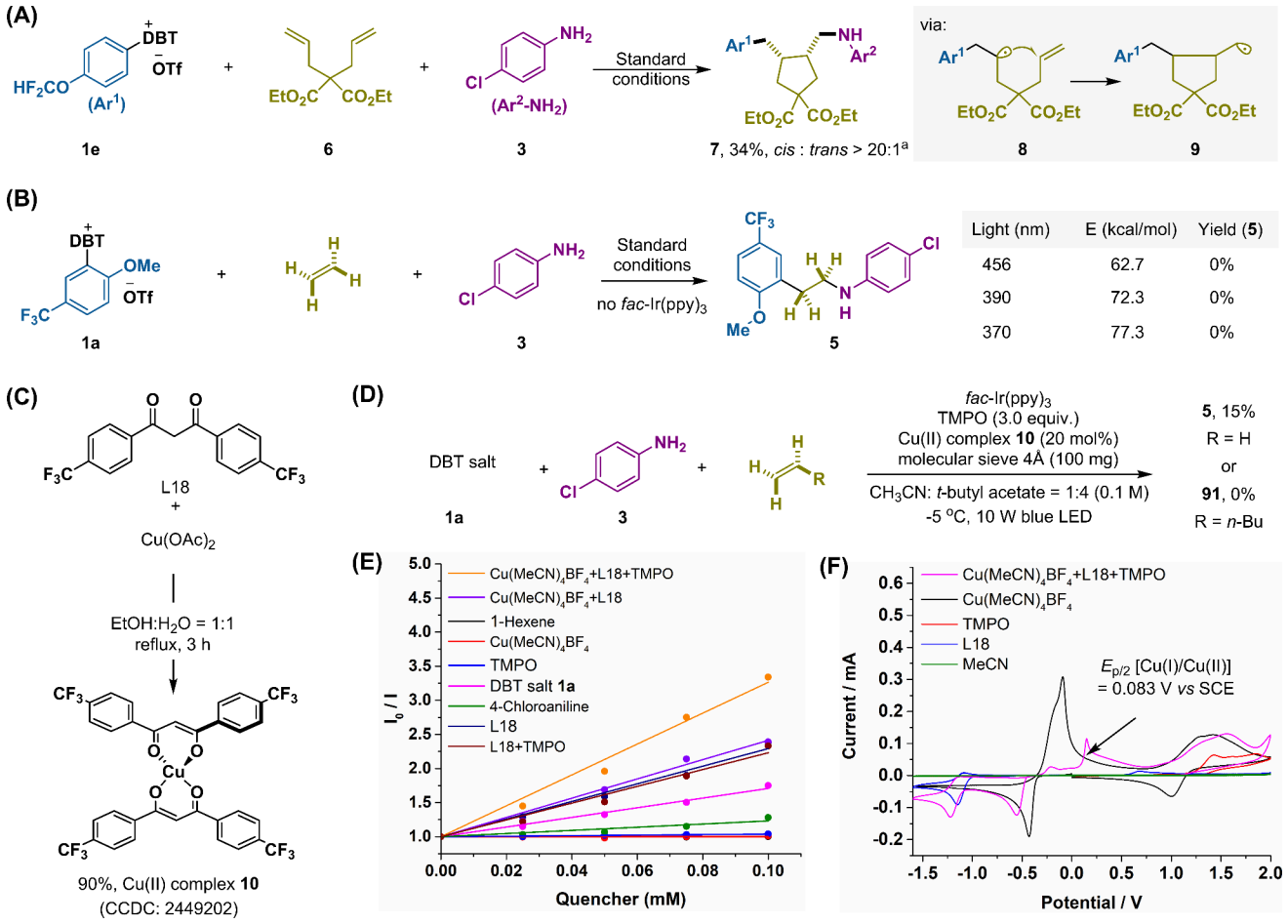

Figure 3. Mechanistic investigations. (A) A radical clock experiment. (B) Reactions under different light sources in the absence of *fac*-Ir(ppy)$_3$. (C) Synthesis of Cu(II) complex **10**. (D) Control experiment using Cu(II) complex **10** as the metal catalyst instead of Cu(MeCN)$_4$BF$_4$ and L18. (E) Stern–Volmer luminescence quenching experiments. (F) Cyclic voltammetry experiments. [a]*cis*/*trans* isomer was determined by H–H COSY and H–H NOESY spectroscopy measurement.

as coupling partners, the same protocol provides a concise and practical route for synthesizing amphetamine and allylamine compounds, which are also important scaffolds in medicinal chemistry.[59]

RESULTS AND DISCUSSION

Reaction Optimization

We initiated our study with aryl dibenzothiophenium salt **1a**, readily prepared from the corresponding arene, as the model substrate for the aminoarylation of ethylene with 4-chloroaniline (**3**) under photoredox/copper dualcatalysis. Given the crucial role of ligands in transition-metal catalyzed cross-coupling reactions, we systematically evaluated a broad set of ligands (Figure 2A). Common neutral and anionic nitrogen-containing bidentate ligands (L1–L6), previously effective in copper-catalyzed C–N couplings, failed to promote the arylamination of ethylene, instead favoring undesired two-component C–N coupling between aryl radicals and arylamines. Likewise, the tridentate nitrogen-based ligands (L7–L11) and the diimine ligand (L12) were unable to deliver the target product. In addition, the bisphosphine ligand 1,1′-binaphthyl-2,2′-diphenylphosphine (BINAP, L13) and the NHC ligand 1,3-bis(2,6-diisopropylphenyl)-4,5-dihydro-1H-imidazol-3-ium chloride (L14) were also ineffective. An encouraging 18% yield of N-aryl-substituted arylethylamine **5** was obtained by using 2,2,6,6-tetramethylheptane-3,5-dione ligand (L15), motivating further exploration of 1,3-diketone ligands (Figure 2B). Ligands bearing electron-withdrawing groups, such as 1,1,1-trifluoropentane-2,4-dione (L16) and 4,4,4-trifluoro-1-phenylbutane-1,3-dione (L17), improved the product yields to 25% and 26%, respectively. Remarkably, the efficiency of this reaction was significantly enhanced with diaryl-substituted 1,3-diketone ligands (L19–L24), culminating in an optimized yield of 65% when 30 mol % of 1,3-bis(4-(trifluoromethyl)phenyl)propane-1,3-dione (L18) was employed (Figure 2B, see Table S1 for details). To probe the role of the dibenzothiophene (DBT) scaffold, alternative aryl sulfonium salts, including 5-(2-methoxy-5-(trifluoromethyl)-phenyl)-5H-thianthren-5-ium trifluoromethanesulfonate **1b** (TT salt) and 10-(2-methoxy-5-(trifluoromethyl)phenyl)-10H-phenoxathiin-10-ium trifluoromethanesulfonate **1c** (PTX salt), were also evaluated under metallaphotoredox conditions. However, both substrates led to diminished yields, highlighting the unique and beneficial role of the DBT-derived salt in this transformation, possibly due to differences in their redox properties and reactivity as aryl radical precursors. Substituting Cu(MeCN)$_4$BF$_4$ with other copper catalysts reduced the yield of aminoarylation product **5** (Figure 2C, entry 2). Replacement of *fac*-Ir(ppy)$_3$ with Ir(dFCF$_3$ppy)$_2$(dtbbpy)PF$_6$, 4CzIPN, or 4DPAIPN, also reduced product formation

https://doi.org/10.1021/jacs.6c03412
J. Am. Chem. Soc. XXXX, XXX, XXX–XXX

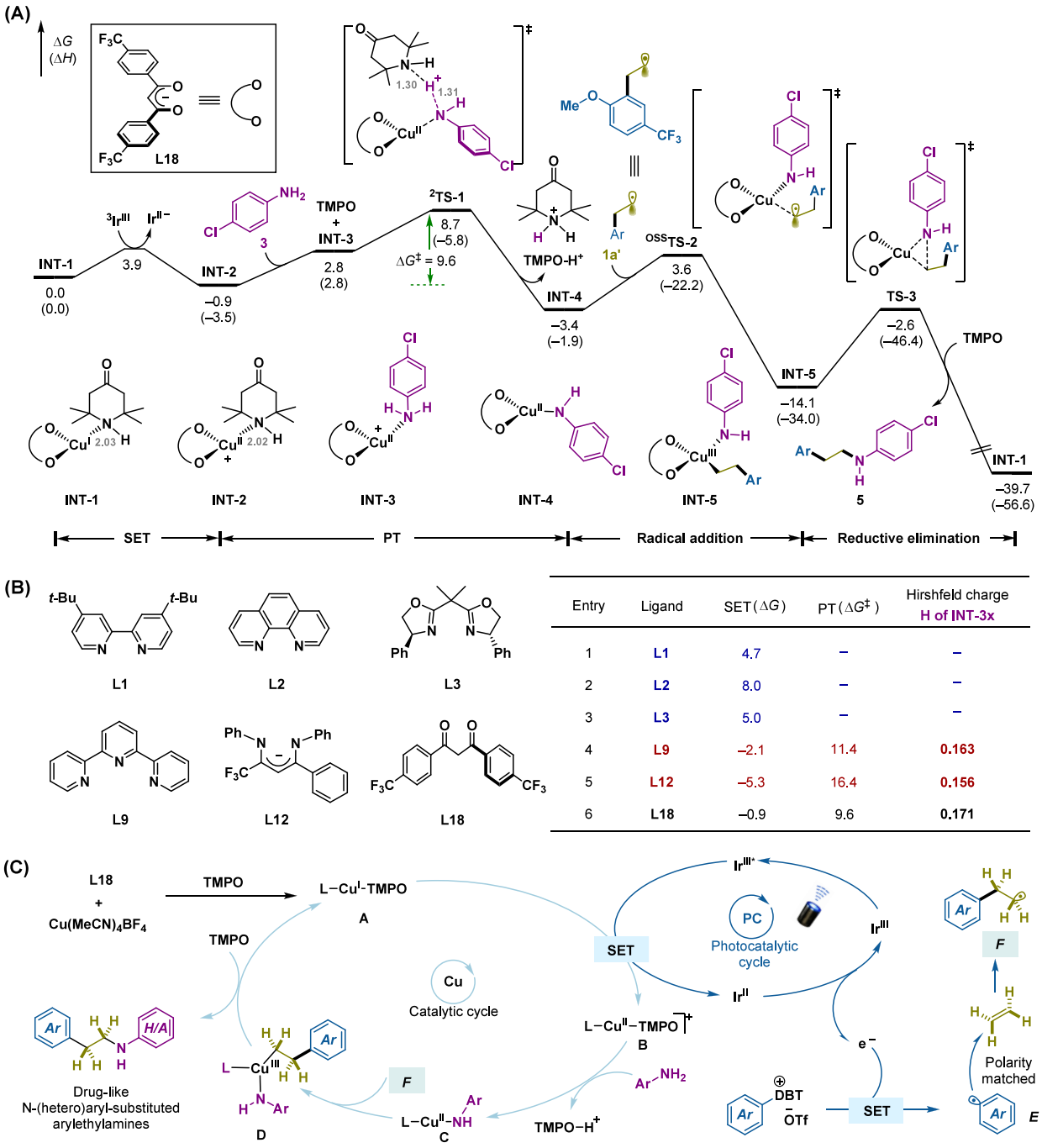

Figure 4. DFT calculations and proposed mechanisms. (A) Free energy profile of the reaction pathway of Cu(I)/L18-catalyzed carboamination. The bidentate ligand used in DFT calculation is 1,3-bis(4-(trifluoromethyl)phenyl)propane-1,3-dione (L18). All energies were calculated at M06-L/6−311+G(d,p)−LANL2TZ(for Cu)−LANL2TZ(f)(for Ir)/SMD(Acetonitrile)//B3LYP-D3(BJ)/6-31G(d)−LANL2DZ (for Cu and Ir)/SMD(Acetonitrile) level of theory. The energies are in kcal/mol. See Figures S6−S8 for details. (B) Computational study of Cu(I)/L-catalyzed process including SET and PT (see Figure S10 for details). (C) Proposed reaction mechanisms.

(entry 3). Reaction conditions such as solvent and temperature were also critical, with variations leading to lower yields ranging from 25% to 57% (entries 4 and 5). When Et_3N, Et_2NH, or DIPEA was used in place of TMPO as the base, no desired product was observed, likely due to hydrogen atom transfer (HAT) between the aryl radical and the α-C−H bonds of the amines,[60,61] which quenches key aryl radical intermediates and suppresses the reaction (entry 6). Omission of TMPO resulted in a significant decrease in yield (entry 7). In the absence of 4 Å molecular sieves, the yield of the desired product dropped sharply, likely due to moisture-induced side reactions or partial catalyst deactivation (entry 8). Additionally, control experiments confirmed that the absence of *fac*-Ir(ppy)$_3$, Cu catalysts or light entirely suppressed product formation, underscoring the indispensability of these components in this reaction (entry 9).

Mechanistic Studies

To gain mechanistic insights into the aminoarylation of ethylene and clarify the role of the diaryl-substituted 1,3-diketone ligand, we carried out a series of control experiments,

https://doi.org/10.1021/jacs.6c03412
J. Am. Chem. Soc. XXXX, XXX, XXX−XXX

spectroscopic investigations, and DFT calculations (Figures 3 and 4). A radical clock experiment using diethyl 2,2-diallylmalonate **6** as the substrate under standard conditions afforded the cyclized product **7** in 34% isolated yield. This result confirms the generation of an aryl radical from DBT salt **1e**, followed by its addition to a terminal alkene, leading to radical intermediate **9** through intramolecular cyclization (Figure 3A). In the absence of photocatalyst *fac*-Ir(ppy)$_3$, no product **5** was formed under irradiation at various wavelengths. These results underscore the crucial role of the photocatalyst in the ethylene carboamination where an energy transfer pathway is highly unlikely (Figure 3B). When Cu(II) complex **10**, which was generated from Cu(OAc)$_2$ and ligand L18 in a EtOH:H$_2$O = 1:1 mixture, was used to substitute Cu(MeCN)$_4$BF$_4$ and L18, the yields of products **5** and **91** were significantly suppressed (Figure 3C and D). Meanwhile, Stern−Volmer luminescence quenching studies revealed that in situ generated diaryl-substituted 1,3-diketone-chelated Cu-complexes exhibited significantly greater quenching of the excited state of *fac*-Ir(ppy)$_3$ compared to DBT salt **1a** and other potential quenchers (Figure 3E). These results provide strong evidence for the preferential interaction between the in situ generated 1,3-diketone-chelated Cu(I) species and the excited photocatalyst. Furthermore, cyclic voltammetry measurements determined the oxidation potential of Cu(I) in the presence of L18 and TMPO to be $E_{p/2}$ = 0.083 V vs SCE, which is lower than that of the excited state Ir(III)* species ($E_{1/2}$ [Ir*(III)/Ir(II)] = 0.31 V vs SCE). This thermodynamic relationship confirms the feasibility of photoinduced electron transfer from Cu(I) to Ir(III)*, enabling the formation of a Cu(II) intermediate while simultaneously reducing Ir(III)* to Ir(II) (Figure 3F).

To further elucidate the role of ligands on the formation of N-aryl-substituted arylethylamines, we performed density functional theory (DFT) calculations.[62,63] Under the experimental conditions, the Cu(MeCN)$_4$BF$_4$ precatalyst can undergo ligand exchange with various coordinating species in the reaction mixture, including the alkali-activated ligand, ArNH$_2$, DBT salt, DBT, TMPO, and CH$_3$CN, giving rise to a range of Cu(I) species. Computational studies indicate that the lowest energy Cu(I) intermediate (**INT-1**), which features coordination of a bidentate L18 ligand together with one TMPO molecule, is chosen as the relative zero point for the computed free energy profiles. (see Figure S7 for details). As shown in Figure 4A, photoexcited *Ir(III) undergoes intersystem crossing to its triplet state, which is reductively quenched by Cu(I) via a SET process, affording ground-state Ir(II) and the cationic Cu(II) species **INT-2** (ΔG = −0.9 kcal/mol). This SET step proceeds readily owing to a low Marcus energy barrier ($\Delta G^{\ddagger}$ = 3.9 kcal/mol). Subsequent displacement of TMPO in **INT-2** by 4-chloroaniline (**3**) furnishes the cationic arylamine-coordinated Cu(II) intermediate **INT-3**, an endergonic process (ΔG = 3.7 kcal/mol). The liberated TMPO acts as a base, facilitating PT via outer-sphere transition state ^{2}**TS-1** ($\Delta G^{\ddagger}$ = 9.6 kcal/mol) to form the Cu(II)-amino intermediate **INT-4**. Alternative stepwise PT ($\Delta G^{\ddagger}$ = 15.3 kcal/mol) and SET ($\Delta G^{\ddagger}$ = 20.1 kcal/mol) pathways were also computed, but their higher barriers render them energetically unfavorable (see Figure S8 for details). Notably, the PT step is irreversible, as formation of **INT-4** is exergonic by 2.5 kcal/mol (reversible to **INT-4** via ^{2}**TS-1**, $\Delta G^{\ddagger}$ = 12.1 kcal/mol). The ensuing radical addition of homobenzylic radical **1a′** to the Cu(II) center of **INT-4** via open-shell singlet transition state ^{OSS}**TS-2** only requires an energy barrier of 7.0 kcal/mol, leading to the highly exergonic formation of alkyl−Cu(III) complex **INT-5**. Subsequent C−N reductive elimination from the alkyl-Cu(III) complex through **TS-3** ($\Delta G^{\ddagger}$ = 16.7 kcal/mol) affords the desired product **5**. Other possible pathways from **INT-4**, including the aryl radical addition to the Cu(II) center (^{OSS}**TS-6**, $\Delta G^{\ddagger}$ = 8.7 kcal/mol), the metal-alkene-coupled (MAC) radical addition pathway (^{OSS}**TS-7**, $\Delta G^{\ddagger}$ = 24.2 kcal/mol),[64] and ethylene migratory insertion into N−Cu(II) bond (**TS-8**, $\Delta G^{\ddagger}$ = 25.7 kcal/mol), all exhibit higher activation barriers than ^{OSS}**TS-2**. These results account for the chemoselective formation of N-(hetero)aryl-substituted arylethylamines in the presence of diaryl-substituted 1,3-diketone ligand L18 (see Figure S9 for details).

To dissect the ligand effects, we further examined the thermodynamic feasibility of Cu(I)-mediated reductive quenching of triplet Ir(III) and the kinetic probability of PT with different ligand frameworks in irreversible stepwise processes (Figure 4B). With neutral bidentate ligands, reductive quenching of triplet Ir(III) by the active cationic Cu(I)-TMPO complex **INT-1x** is endergonic by 4.7 kcal/mol (L1), 8.0 kcal/mol (L2), and 5.0 kcal/mol (L3), reflecting the poor stability of the resulting dicationic Cu(II)−TMPO species **INT-2x** and rendering the process thermodynamically unfavorable. Furthermore, tridentate ligand (L9) and anionic ligand (L12) significantly stabilize the dicationic/cationic Cu(II)-TMPO complex **INT-2x** via increased coordination sites (L9) and enhanced electronegativity (L12). Although the initial SET step is thermodynamically feasible, the subsequent PT step requires activation barriers of 11.4 kcal/mol (L9) and 16.4 kcal/mol (L12), respectively, which are 1.8 kcal/mol (L9) and 6.8 kcal/mol (L12) higher than that observed with the 1,3-diketone ligand L18 ($\Delta G^{\ddagger}$ = 9.6 kcal/mol). Hirshfeld charge analysis of the transferring H atom in the cationic ArNH$_2$−Cu(II) complex **INT-3x** (0.171 for L18, 0.163 for L9, and 0.156 for L12) indicates that the ligand-stabilized Cu(II) center modulates N−H bond acidity, thereby influencing the feasibility of proton transfer (see Figure S10 for details).

On the basis of experimental mechanistic studies and DFT calculations, a plausible pathway for the copper/photoredox-catalyzed aminoarylation of ethylene is proposed (Figure 4C). Visible-light excitation of the photocatalyst *fac*-Ir(ppy)$_3$ generates triplet Ir(III) via intersystem crossing, which undergoes reductive quenching by the TMPO-coordinated Cu(I) species **A** through a SET event, affording the cationic Cu(II) intermediate **B** along with reduced Ir(II). Subsequent displacement of TMPO in the cationic L−Cu(II)−TMPO complex **B** by an arylamine activates the free N−H bond of Ar−NH$_2$ at the Cu(II) center, while TMPO acts as a base to mediate proton transfer, yielding the Cu(II)-amino species **C**. The homobenzylic radical **F**, formed via radical addition of aryl radical **E** to ethylene (with **E** originating from reduction of the DBT salt by Ir(II)), then adds to Cu(II) species **C** to form alkyl-copper(III) species **D**.[65] Reductive elimination from intermediate **D** delivers the N-(hetero)aryl-substituted arylethylamine products, with concurrent coordination of TMPO to the Cu(I) center regenerating active catalyst **A** and closing the catalytic cycle.

Substrate Scope

Having established the optimized conditions, we next explored the substrate scope, with an initial examination of variety of arylamine nucleophiles. Notably, our protocol exhibited

https://doi.org/10.1021/jacs.6c03412
J. Am. Chem. Soc. XXXX, XXX, XXX−XXX

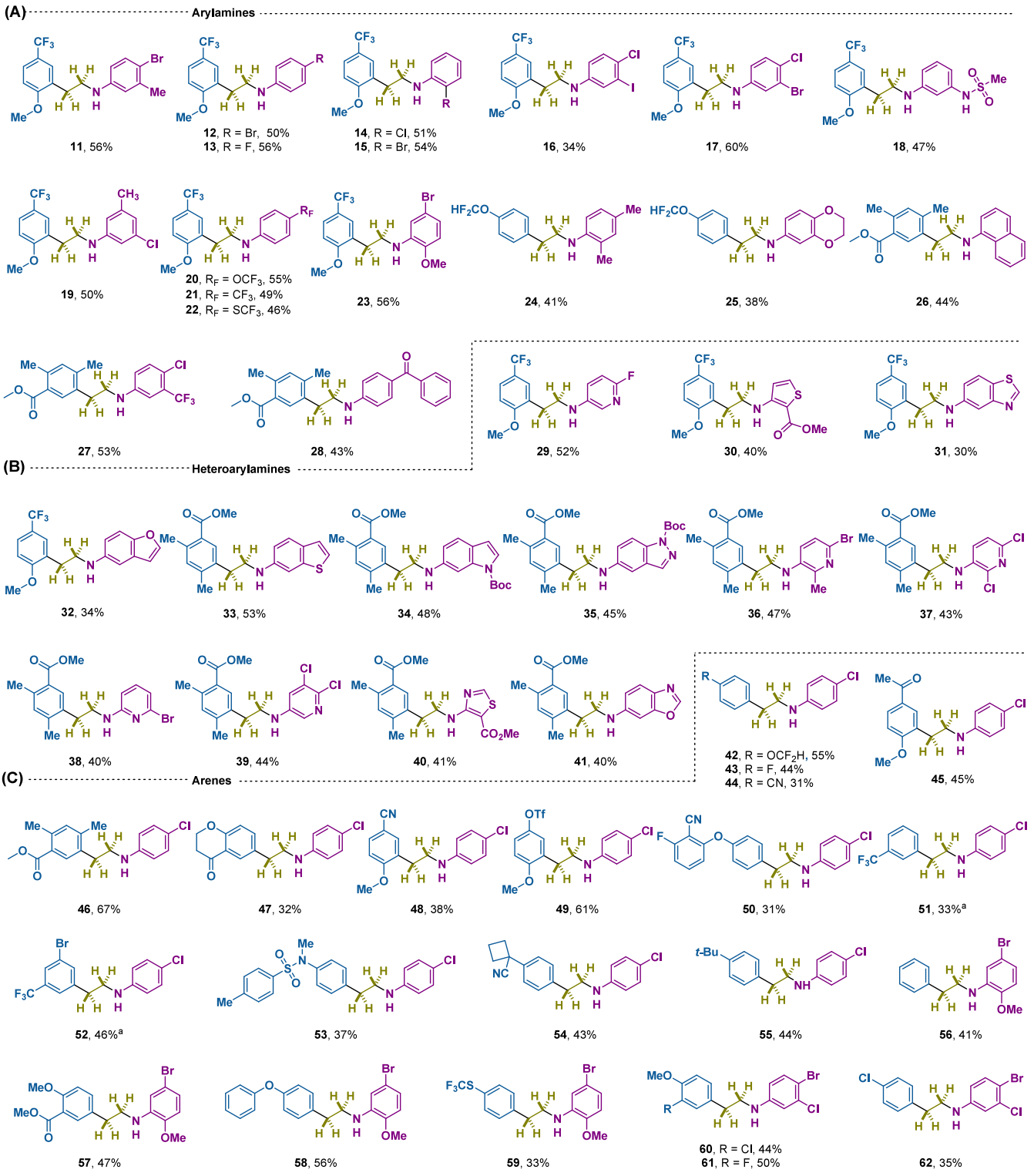

Figure 5. Substrate scope of ethylene difunctionalization with unprotected (hetero)arylamines and arenes. (A) Substrate scope of arylamines. (B) Substrate scope of heteroarylamines. (C) Substrate scope of arenes. All reactions were carried out with DBT salts (0.10 mmol), (hetero)arylamines (2.0 equiv), TMPO (3.0 equiv), $Cu(MeCN)_4BF_4$ (20 mol %), L18 (30 mol %), molecular sieve 4Å (100 mg), *fac*-Ir(ppy)$_3$ (2 mol %), 60 mL of ethylene in MeCN/*t*-BuOAc (1:4, 0.1 M) at −5 °C under 10 W 456 nm LED light irradiation in a 10 mL microwave tube.

remarkable adaptability in bridging diverse arylamine motifs with aromatic hydrocarbons via ethylene as a C2 synthon (Figure 5). Arylamines featuring halogen substituents (F, Cl, Br, I) at different positions on the aromatic ring performed well to deliver N-aryl-substituted arylethylamine products **12**-**17** in moderate to good yields, providing versatile handles for subsequent functionalization. Polysubstituted arylamines also efficiently yield the target products (**11**, **19**, **23**). Furthermore, arylamines containing fluorinated groups, which are prevalent in pharmaceuticals and bioactive molecules, such as trifluoromethoxy (**20**), trifluoromethyl (**21**, **27**), trifluoromethylthio (**22**), difluoromethoxy (**24**), underwent smooth transforma-

https://doi.org/10.1021/jacs.6c03412
J. Am. Chem. Soc. XXXX, XXX, XXX−XXX

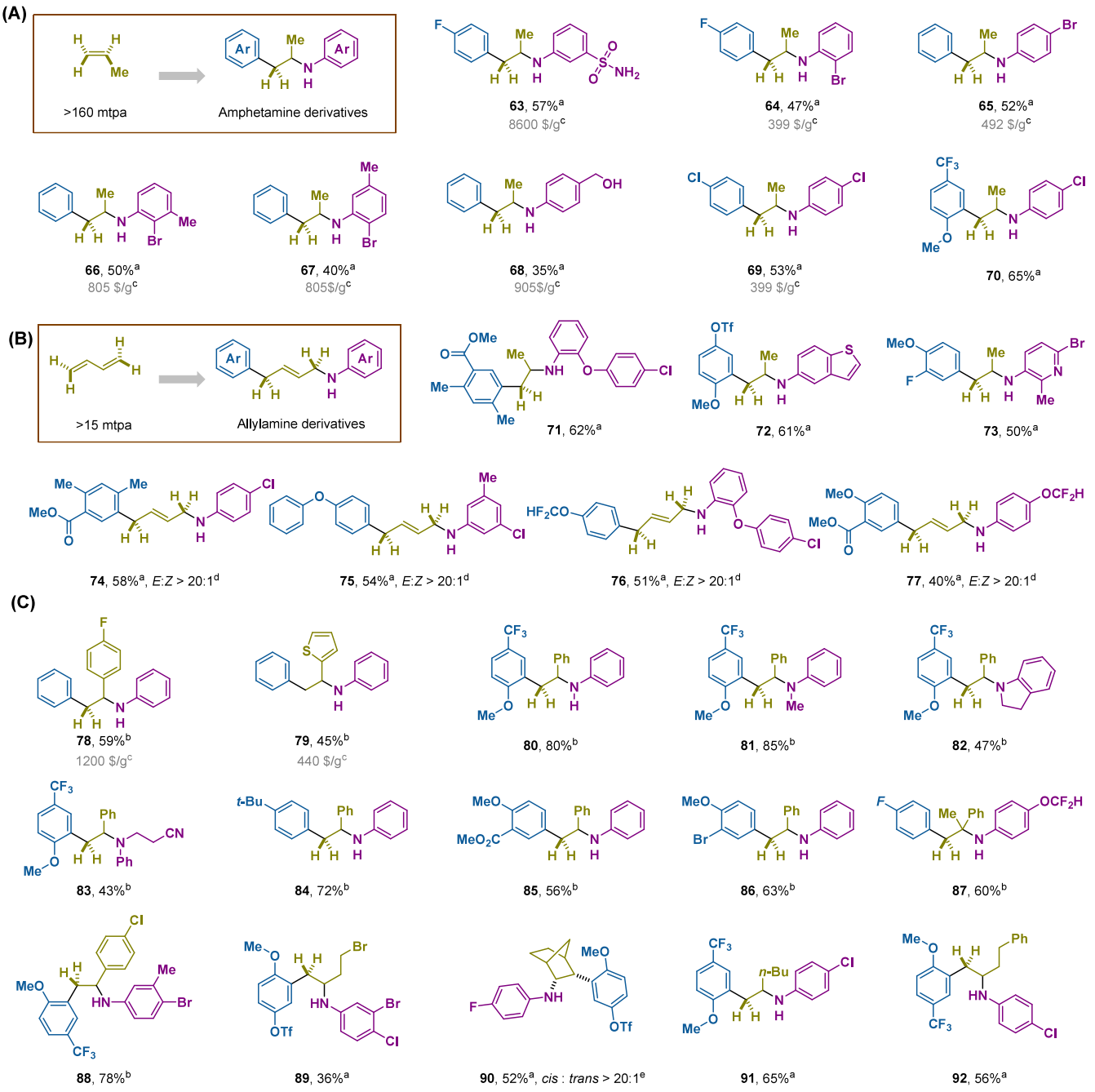

Figure 6. Substrate scope with propylene, 1,3-butadiene, and nongaseous alkenes. (A) Synthesis of amphetamine derivatives using propylene. (B) Synthesis of allylamine derivatives using 1,3-butadiene. (C) Aminoarylation of nongaseous alkenes. [a]DBT salts (0.10 mmol), (hetero)arylamines (2.0 equiv), TMPO (3.0 equiv), $Cu(MeCN)_4BF_4$ (20 mol %), L18 (30 mol %), molecular sieve 4Å (100 mg), *fac*-$Ir(ppy)_3$ (2 mol %), 60 mL of propylene (or 10 equiv of nongaseous alkenes or 1,3-butadiene in *n*-hexane were used) in MeCN/*t*-BuOAc (1:4, 0.1 M) at −5 °C under 10 W 456 nm LED light irradiation in a 10 mL microwave tube. [b]DBT salts (0.10 mmol), (hetero)arylamines (2.5 equiv), alkenes (5.0 equiv), $KHCO_3$ (4.0 equiv), $Cu(CF_3COO)_2 \bullet H_2O$ (20 mol %), molecular sieve 4Å (100 mg), *fac*-$Ir(ppy)_3$ (2 mol %) in DCM/Ph−CF_3 (1:1, 0.1 M) at 5 °C under 10 W 456 nm LED light irradiation. [c]The product price was sourced from the Reaxys database in April 2025. [d]*E*/*Z* isomers were determined by ^1H NMR spectroscopy measurement of the crude reaction mixture. [e]*cis*/*trans* isomer was determined by H−H COSY and H−H NOESY spectroscopy measurement.

tions, affording the coupling products in good yields. The mild conditions further enabled broad functional group tolerance, accommodating ethers (**18**), sulfonamides (**25**), naphthyl units (**26**), ketones (**28**), and esters (**30**). Additionally, heteroaryl amines, including those derived from pyridine (**29**, **36**−**39**), thiophene (**30**), benzothiazole (**31**), benzofuran (**32**), benzothiophene (**33**), indole (**34**), indazole (**35**), thiazole (**40**), and benzoxazole (**41**), could also furnish the target N-heteroaryl-substituted arylethylamine products with moderate yields, underscoring its significant potential for pharmaceutical synthesis (Figure 5B).

We next evaluated the substrate scope of diverse arenes by employing aryl dibenzothiophenium salts as aryl radical precursors. This ligand-modulated copper/photoredox-cata-

https://doi.org/10.1021/jacs.6c03412
J. Am. Chem. Soc. XXXX, XXX, XXX−XXX

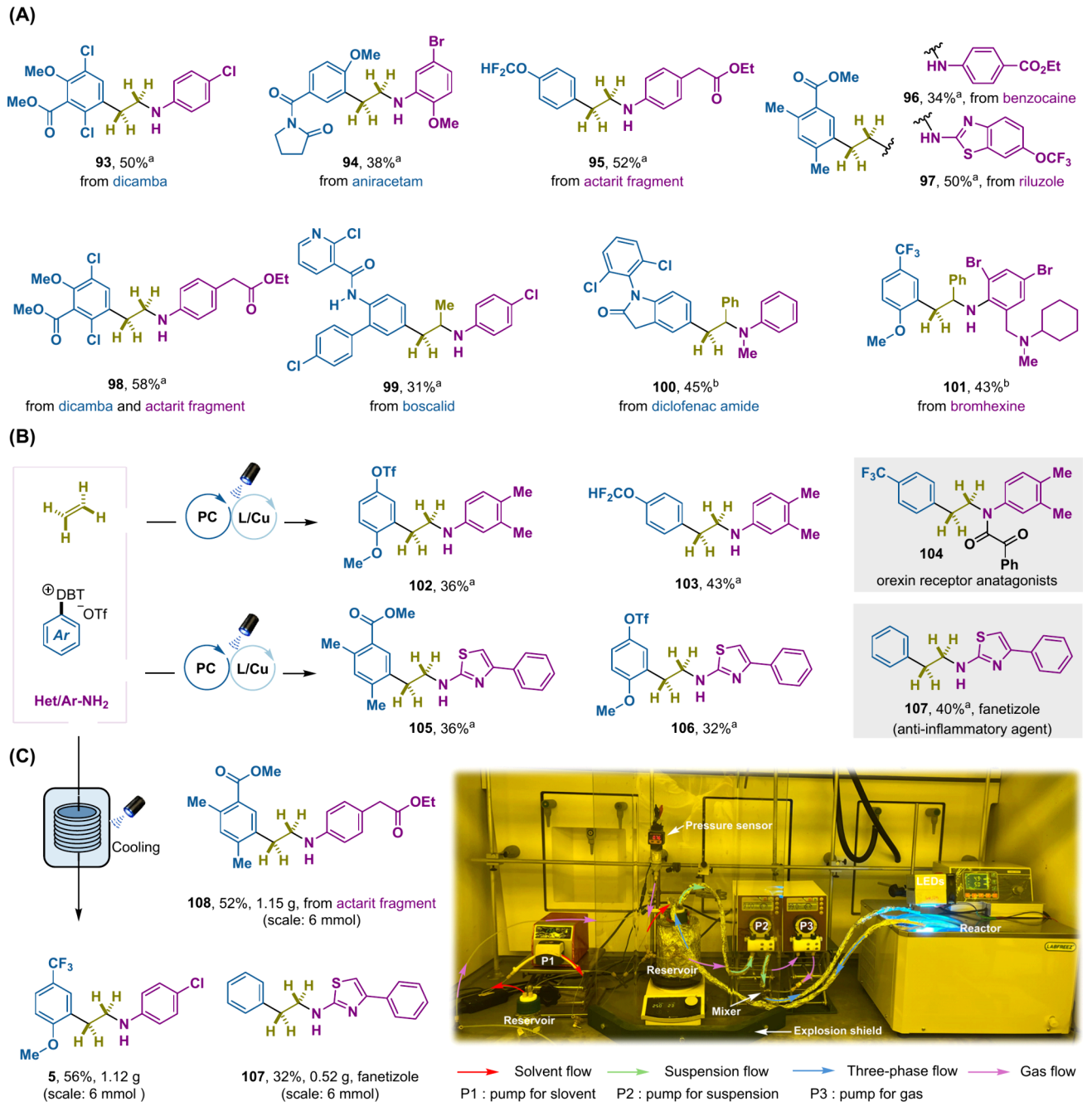

Figure 7. Synthetic applications. (A) Late-stage modification of drug molecules and agrochemicals. (B) Synthesis of bioactive molecules and analogues. (C) Scaling up by a circulation-flow reactor (picture taken with a yellow filter for clarity). [a]DBT salts (0.10 mmol), (hetero)arylamines (2.0 equiv), TMPO (3.0 equiv), $Cu(MeCN)_4BF_4$ (20 mol %), L18 (30 mol %), molecular sieve 4Å (100 mg), *fac*-Ir(ppy)$_3$ (2 mol %), 60 mL of ethylene in MeCN/*t*-BuOAc (1:4, 0.1 M) at −5 °C under 10 W 456 nm LED light irradiation in a 10 mL microwave tube. [b]DBT salts (0.10 mmol), (hetero)arylamines (2.5 equiv), alkenes (5.0 equiv), $KHCO_3$ (4.0 equiv), $Cu(CF_3COO)_2{\cdot}H_2O$ (20 mol %), molecular sieve 4Å (100 mg), *fac*-Ir(ppy)$_3$ (2 mol %) in DCM/Ph−CF_3 (1:1, 0.1 M) at 5 °C under 10 W 456 nm LED light irradiation.

lyzed three- component cross-coupling protocol exhibited broad applicability across a wide range of aromatic hydrocarbons, resulting in the efficient synthesis of N-aryl-substituted arylethylamine with good yields (Figure 5C). Arenes bearing both electron-donating and electron-withdrawing substituents, as well as ortho-, meta-, and para-substitution patterns, were readily accommodated, affording N-aryl-substituted arylethylamine products in moderate to good yields. Notably, the protocol demonstrated exceptional functional group compatibility, including difluoromethoxy (**42**), halogens (F, Cl, Br) (**43**, **52**, **60**, **61**, **62**), nitriles (**44**, **48**), ketones (**45**, **47**), esters (**46**), triflates (**49**), ethers (**50**, **58**), trifluoromethyl (**51**), sulfonamides (**53**), trifluoromethylthio (**59**), and strained cyclobutyl motifs (**54**).

To further assess the generality of this catalytic method, a broad range of readily accessible alkene substrates were investigated (Figure 6). Propylene, a major petrochemical feedstock (>160 mtpa in 2023) and key intermediate in the production of bulk chemicals such as propylene oxide (for polyurethane foams) and acrylonitrile (for synthetic fibers and

https://doi.org/10.1021/jacs.6c03412
J. Am. Chem. Soc. XXXX, XXX, XXX−XXX

plastics), remains underutilized in fine chemical synthesis. Remarkably, this modular three-component coupling strategy was successfully extended to propylene in a highly regioselective manner, enabling the synthesis of value-added amphetamine derivatives with good functional group tolerance (**63**−**73**). This transformation highlights the synthetic flexibility of the method, allowing diverse arenes and (hetero)arylamines to be efficiently cross-coupled using propylene. Furthermore, 1,3-butadiene, the most economically important unsaturated C4 hydrocarbon with global production of 15 million tons in 2023,[66] undergoes mild carboamination via diaryl-substituted 1,3-diketone-regulated metallaphotoredox catalysis to furnish allylamines (**74**−**77**) with excellent *E*-stereoselectivity. These motifs, commonly found in pharmaceuticals and natural products, underscore the synthetic utility of this method. Notably, the methodology was also extended to nongaseous alkenes to generate valuable coupling products (**78**−**79**). Secondary amines were compatible with the vicinal aminoarylation to deliver the desired products (**81**−**83**). Activated alkenes, like styrene and its derivatives, readily participated in the photoredox/copper dual-catalyzed process, resulting in the formation of aminoarylation products in high yields (**80**, **84**−**88**). Additionally, unactivated alkenes, including both terminal and internal olefins, were effectively incorporated into the three-component coupling, furnishing the corresponding products in moderate to good yields (**89**−**92**). These results collectively demonstrate the broad applicability and robustness of this modular aminoarylation platform across diverse alkene classes.

Further Synthetic Applications

Late-stage functionalization (LSF) provides a concise approach for the rapid diversification of complex molecular architectures and the generation of molecular libraries. Given the mild conditions and exceptional functional group tolerance of our methodology, we applied it to the late-stage modification of pharmaceuticals and agrochemicals, as well as the direct synthesis of bioactive molecules (Figure 7). In these studies, the biologically relevant molecules were first converted into the corresponding aryldibenzothiophenium salts via regioselective arene C−H sulfonium salt formation, which proceeded efficiently and with high site selectivity. Aryl radical precursors derived from drug molecules, such as dicamba (**93**), aniracetam (**94**), boscalid (**99**), diclofenac amide (**100**), underwent efficient transformations to furnish the corresponding coupling products in moderate to good yields. Moreover, pharmaceuticals bearing free N−H group, such as actarit fragment (**95**), benzocaine (**96**), riluzole (**97**), bromhexine (**101**), were also successfully employed in alkene aminoarylation to afford the drug-like N-(hetero)aryl-substituted arylethylamine derivatives. The synthetic utility of this methodology was further showcased by synthesizing two types of bioactive molecules, including orexin receptor anatagonist fragments[67] (**102**, **103**) and fanetizole (**107**), an immunomodulatory drug.[6] Flow technology is increasingly favored in photochemical synthesis because of its enhanced safety, improved efficiency, scalability, and superior light penetration.[68] To demonstrate the scalability and practical utility of the methodology, we employed a circulation-flow photoreactor for gas/liquid/solid three-phase photochemical reactions,[69] achieving the gram-scale synthesis of N-(hetero)-aryl-substituted arylethylamine products (**5**, **107**, **108**). Unlike classic continuous flow systems, which often suffer from clogging and poor handling of solid or viscous reaction mixtures, our approach demonstrates excellent tolerance of solid reagents, enabling efficient processing of heterogeneous photoreactions.

CONCLUSIONS

In summary, we have developed a ligand-regulated metallaphotoredox aminoarylation of ethylene that enables the direct synthesis of N-(hetero)aryl-substituted arylethylamine derivatives from commercially available arenes and unprotected (hetero)arylamines. The success of this photoredox/copper dual-catalyzed three-component coupling relies on the usage of diaryl-substituted 1,3-diketone ligands, which finely modulate the SET and PT steps to enable efficient aminoarylation of ethylene. This modular approach features a broad substrate scope encompassing pharmaceutical and natural product motifs, along with exceptional functional group tolerance, highlighting its utility for late-stage functionalizations to access drug-like scaffolds. Furthermore, this method can be extended to propylene, 1,3-dienes, and nongaseous alkenes, allowing access to a diverse array of biologically relevant scaffolds such as amphetamine and allylamine derivatives, further underscoring its versatility in generating molecular diversity from abundant chemical feedstocks.

ASSOCIATED CONTENT

Supporting Information

The Supporting Information is available free of charge at https://pubs.acs.org/doi/10.1021/jacs.6c03412.

General procedures, reaction optimization tables, analytical data, details of DFT calculations, and characterization data for all the products (PDF)

Accession Codes

Deposition Number 2449202 contains the supplementary crystallographic data for this paper. These data can be obtained free of charge via the joint Cambridge Crystallographic Data Centre (CCDC) and Fachinformationszentrum Karlsruhe Access Structures service.

AUTHOR INFORMATION

Corresponding Authors

Yixin Luo − *State Key Laboratory of Antiviral Drugs, Pingyuan Laboratory, Henan Normal University, Xinxiang, Henan 453007, P. R. China*; Email: luoyixin@htu.edu.cn

Yu Lan − *College of Chemistry, and Pingyuan Laboratory, Zhengzhou University, Zhengzhou, Henan 450001, P. R. China; State Key Laboratory of Antiviral Drugs, Pingyuan Laboratory, Henan Normal University, Xinxiang, Henan 453007, P. R. China; Chongqing Key Laboratory of Chemical Theory and Mechanism, Chongqing University, Chongqing 401331, P. R. China*; orcid.org/0000-0002-2328-0020; Email: LanYu@cqu.edu.cn

Jie Wu − *Department of Chemistry, National University of Singapore, Singapore 117543, Republic of Singapore; National University of Singapore (Suzhou) Research Institute, Suzhou, Jiangsu 215123, P. R. China*; orcid.org/0000-0002-9865-180X; Email: chmjie@nus.edu.sg

https://doi.org/10.1021/jacs.6c03412
J. Am. Chem. Soc. XXXX, XXX, XXX−XXX

Authors

Weigang Zhang − *Department of Chemistry, National University of Singapore, Singapore 117543, Republic of Singapore;* orcid.org/0009-0000-3617-916X

Zhexuan Lei − *Department of Chemistry, National University of Singapore, Singapore 117543, Republic of Singapore*

Tao Liu − *Department of Chemistry, National University of Singapore, Singapore 117543, Republic of Singapore*

Xiao Guo − *Department of Chemistry, National University of Singapore, Singapore 117543, Republic of Singapore*

Jiahe Shen − *Department of Chemistry, National University of Singapore, Singapore 117543, Republic of Singapore*

Jianke Su − *Department of Chemistry, National University of Singapore, Singapore 117543, Republic of Singapore*

Yan Li − *Department of Chemistry, National University of Singapore, Singapore 117543, Republic of Singapore*

Jiale Wu − *Department of Chemistry, National University of Singapore, Singapore 117543, Republic of Singapore*

Hong Jiang − *Department of Chemistry, National University of Singapore, Singapore 117543, Republic of Singapore*

Hwee Ting Ang − *Department of Chemistry, National University of Singapore, Singapore 117543, Republic of Singapore;* orcid.org/0000-0001-6124-1463

Xingwei Guo − *Center for Advanced Light Source and Department of Chemistry, Southern University of Science and Technology, Shenzhen 518055, P. R. China;* orcid.org/0000-0002-5461-0360

Complete contact information is available at: https://pubs.acs.org/10.1021/jacs.6c03412

Notes

The authors declare no competing financial interest.

■ ACKNOWLEDGMENTS

We are grateful for the financial support provided by the National Research Foundation, the Prime Minister's Office of Singapore, under its NRF-CRP Programme (Award NRFCRP25-2020RS-0002), the Ministry of Education (MOE) of Singapore (MOET2EP10224-0005), NUS (Suzhou) Research Institute, Science and Technology Project of Jiangsu Province (BZ2022056), National Natural Science Foundation of China (Grant Nos. 22371200, 22531008), and Henan Scientific and Technological Research Project (Grant 252102310388).

■ REFERENCES

(1) Wang, J.; Hou, T. Drug and drug candidate building block analysis. *J. Chem. Inf. Model.* **2010**, *50*, 55−67.

(2) Pozhydaiev, V.; Muller, C.; Moran, J.; Lebœuf, D. Catalytic synthesis of *β*-(hetero)arylethylamines: modern strategies and advances. *Angew. Chem., Int. Ed.* **2023**, *62*, No. e202309289.

(3) Nieto, C. T.; Manchado, A.; Belda, L.; Diez, D.; Garrido, N. M. 2-Phenethylamines in medicinal chemistry: A review. *Molecules* **2023**, *28*, 855.

(4) Bunescu, A.; Abdelhamid, Y.; Gaunt, M. J. Multicomponent alkene azidoarylation by anion-mediated dual catalysis. *Nature* **2021**, *598*, 597−603.

(5) Lee, S.; Song, W.-J.; Park, J.; Kim, M.; Choen, S.; Kim, M.-C.; Jeong, H.; Yun, Y. Off-label use of crisdesalazine (GedaCure) in meningoencephalitis in two dogs. *Vet. Sci.* **2023**, *10*, 438.

(6) Ni, P. H.; Tan, J.; Li, R.; Huang, H.; Zhang, F.; Deng, G.-J. Brønsted acid-promoted thiazole synthesis under metal-free conditions using sulfur powder as the sulfur source. *RSC Adv.* **2020**, *10*, 3931.

(7) Ghanim, M.; Lebedev, G.; Kontsedalov, S.; Ishaaya, I. Flufenerim, a novel insecticide acting on diverse insect pests: Biological mode of action and biochemical aspects. *J. Agric. Food Chem.* **2011**, *59*, 2839−2844.

(8) Chen, Y.; He, R.; Song, H.; Yu, G.; Li, C.; Liu, Y.; Wang, Q. Two-step protocol for iodotrimethylsilane-mediated deoxy-functionalization of alcohols. *Eur. J. Org. Chem.* **2021**, *2021*, 1179−1183.

(9) Romera, J. L.; Cid, J. M.; Trabanco, A. A. Potassium iodide catalysed monoalkylation of anilines under microwave irradiation. *Tetrahedron Lett.* **2004**, *45*, 8797−8800.

(10) Guo, D.; Huang, H.; Zhou, Y.; Xu, J.; Jiang, H.; Chen, K.; Liu, H. Ligand-free iron/copper cocatalyzed *N*-arylations of aryl halides with amines under microwave irradiation. *Green Chem.* **2010**, *12*, 276−281.

(11) Park, S.-E.; Kang, S. B.; Jung, K.-J.; Won, J.-E.; Lee, S.-G.; Yoon, Y.-J. Efficient palladium-catalyzed amination of aryl chlorides using dicyclohexylamino[(2,6-dimethyl)morpholino]phenylphosphine as a PN2 ligand. *Synthesis* **2009**, *2009*, 815−823.

(12) Tao, C. Z.; Liu, W.-W.; Sun, J.-Y.; Cao, Z.-L.; Li, H.; Zhang, Y.-F. 3-Acetylcoumarin as a practical ligand for copper-catalyzed C-N coupling reactions at room temperature. *Synthesis* **2010**, *2010*, 1280−1284.

(13) Purkait, N.; Kervefors, G.; Linde, E.; Olofsson, B. Regiospecific *N*-arylation of aliphatic amines under mild and metal-free reaction conditions. *Angew. Chem., Int. Ed.* **2018**, *57*, 11427−11431.

(14) Han, Y.; Zhang, M.; Zhang, Y.-Q.; Zhang, Z.-H. Copper immobilized at a covalent organic framework: an efficient and recyclable heterogeneous catalyst for the Chan-Lam coupling reaction of aryl boronic acids and amines. *Green Chem.* **2018**, *20*, 4891−4900.

(15) Vantourout, J. C.; Law, R. P.; Isidro-Llobet, A.; Atkinson, S. J.; Watson, A. J. B. Chan-Evans-Lam Amination of boronic acid pinacol (BPin) esters: overcoming the aryl amine problem. *J. Org. Chem.* **2016**, *81*, 3942−3950.

(16) Li, P.; Lee, B. C.; Zhang, X.; Koh, M. J. Base-mediated site-selective hydroamination of alkenes. *Synthesis* **2022**, *54*, 1566−1576.

(17) Gök, Y.; Yiğit, B.; Özeroğlu Çelikal, Ö.; Yiğit, M. AntiMarkovnikov hydroaminations of styrene catalyzed by palladium-(II) N-heterocyclic carbene complexes under conventional and microwave heating. *Transition Met. Chem.* **2018**, *43*, 591−596.

(18) Meena, P.; Ayushee; Patel, M.; Verma, A. K. Transition-metal-free regioselective hydroamination of styrenes with amino-heteroarenes. *Chem. Commun.* **2022**, *58*, 8424−8427.

(19) Sabharwal, G.; Dwivedi, K. C.; Balakrishna, M. S. Multifunctional PNN-Ni^{II} pincer catalyst for C-C and C-N bond formation via alkylation, crosscoupling, and hydroamination reactions. *Catal. Sci. Technol.* **2025**, *15*, 5275−5284.

(20) Lui, E. K. J.; Schafer, L. L. Facile synthesis and isolation of secondary amines *via* a sequential titanium(IV)-catalyzed hydroamination and palladium-catalyzed hydrogenation. *Adv. Synth. Catal.* **2016**, *358*, 713−718.

(21) Sorribes, I.; Cabrero-Antonino, J. R.; Vicent, C.; Junge, K.; Beller, M. Catalytic *N*-alkylation of amines using carboxylic acids and molecular hydrogen. *J. Am. Chem. Soc.* **2015**, *137*, 13580−13587.

(22) Sorribes, I.; Junge, K.; Beller, M. Direct catalytic *N*-alkylation of amines with carboxylic acids. *J. Am. Chem. Soc.* **2014**, *136*, 14314−14319.

(23) Saini, V.; Stokes, B. J.; Sigman, M. S. Transition-metal-catalyzed laboratory-scale carbon-carbon bond-forming reactions of ethylene. *Angew. Chem., Int. Ed.* **2013**, *52*, 11206−11220.

(24) Juliá, F.; Yan, J.; Paulus, F.; Ritter, T. Vinyl thianthrenium tetrafluoroborate: A practical and versatile vinylating reagent made from ethylene. *J. Am. Chem. Soc.* **2021**, *143*, 12992−12998.

(25) Zhang, Y.; Zhou, G.; Gong, X.; Guo, Z.; Qi, X.; Shen, X. Diastereoselective transfer of tri(di)fluoroacetylsilanes-derived carbenes to alkenes. *Angew. Chem., Int. Ed.* **2022**, *61*, No. e202202175.

(26) Matsubara, R.; Gutierrez, A. C.; Jamison, T. F. Nickel-catalyzed Heck-type reactions of benzyl chlorides and simple olefins. *J. Am. Chem. Soc.* **2011**, *133*, 19020−19023.
(27) RajanBabu, T. V. Asymmetric hydrovinylation reaction. *Chem. Rev.* **2003**, *103*, 2845−2860.
(28) Scott, S. C.; Cadge, J. A.; Boden, G. K.; Bower, J. F.; Russell, C. A. A hemilabile NHC-gold complex and its application to the redox neutral 1,2-oxyarylation of feedstock alkenes. *Angew. Chem., Int. Ed.* **2023**, *62*, No. e202301526.
(29) Aukland, M. H.; Šiaučiulis, M.; West, A.; Perry, G. J. P.; Procter, D. J. Metal-free photoredox-catalysed formal C-H/C-H coupling of arenes enabled by interrupted Pummerer activation. *Nat. Catal.* **2020**, *3*, 163−169.
(30) Dewanji, A.; van Dalsen, L.; Rossi-Ashton, J. A.; Gasson, E.; Crisenza, G. E. M.; Procter, D. J. A general arene C-H functionalization strategy via electron donor-acceptor complex photoactivation. *Nat. Chem.* **2023**, *15*, 43−52.
(31) Ye, F.; Berger, F.; Jia, H.; Ford, J.; Wortman, A.; Borgel, J.; Genicot, C.; Ritter, T. Aryl sulfonium salts for site-selective late-stage trifluoromethylation. *Angew. Chem., Int. Ed.* **2019**, *58*, 14615−14619.
(32) Chen, X.-Y.; Nie, X.-X.; Wu, Y.; Wang, P. *para*-Selective arylation and alkenylation of monosubstituted arenes using thianthrene S-oxide as a transient mediator. *Chem. Commun.* **2020**, *56*, 5058−5061.
(33) Alvarez, E. M.; Karl, T.; Berger, F.; Torkowski, L.; Ritter, T. Late-stage heteroarylation of hetero(aryl)sulfonium salts activated by α-amino alkyl radicals. *Angew. Chem., Int. Ed.* **2021**, *60*, 13609−13613.
(34) Meng, H.; Liu, M.-S.; Shu, W. Organothianthrenium salts: synthesis and utilization. *Chem. Sci.* **2022**, *13*, 13690−13707.
(35) Großkopf, J.; Gopatta, C.; Martin, R. T.; Haseloer, A.; MacMillan, D. W. C. Generalizing arene C-H alkylations by radical-radical cross-coupling. *Nature* **2025**, *641*, 112−121.
(36) Harper, M. J.; Emmett, E. J.; Bower, J. F.; Russell, C. A. Oxidative 1,2-difunctionalization of ethylene *via* gold-catalyzed oxyarylation. *J. Am. Chem. Soc.* **2017**, *139*, 12386−12389.
(37) Chatani, N.; Asaumi, T.; Yorimitsu, S.; Ikeda, T.; Kakiuchi, F.; Murai, S. $Ru_3(CO)_{12}$-catalyzed coupling reaction of sp^3 C-H bonds adjacent to a nitrogen atom in alkylamines with alkenes. *J. Am. Chem. Soc.* **2001**, *123*, 10935−10941.
(38) Ohashi, M.; Shirataki, H.; Kikushima, K.; Ogoshi, S. Nickel-catalyzed formation of fluorine-containing ketones *via* the selective cross-trimerization reaction of tetrafluoroethylene, ethylene, and aldehydes. *J. Am. Chem. Soc.* **2015**, *137*, 6496−6499.
(39) Whitehurst, W. G.; Kim, J.; Koenig, S. G.; Chirik, P. J. Three-component coupling of arenes, ethylene, and alkynes catalyzed by a cationic bis(phosphine) cobalt complex: intercepting metallacyclopentenes for C-H functionalization. *J. Am. Chem. Soc.* **2022**, *144*, 4530−4540.
(40) Li, J.; Luo, Y.; Cheo, H. W.; Lan, Y.; Wu, J. Photoredox-catalysis-modulated, nickel-catalyzed divergent difunctionalization of ethylene. *Chem.* **2019**, *5*, 192−203.
(41) Saini, V.; Sigman, M. S. Palladium-catalyzed 1,1-difunctionalization of ethylene. *J. Am. Chem. Soc.* **2012**, *134*, 11372−11375.
(42) Liu, T.; Li, T.; Tea, Z. Y.; Wang, C.; Shen, T.; Lei, Z.; Chen, X.; Zhang, W.; Wu, J. Modular assembly of arenes, ethylene and heteroarenes for the synthesis of 1,2-arylheteroaryl ethanes. *Nat. Chem.* **2024**, *16*, 1705−1714.
(43) Yu, J.; Zhang, X.; Wu, X.; Liu, T.; Zhang, Z.-Q.; Wu, J.; Zhu, C. Metal-free radical difunctionalization of ethylene. *Chem.* **2023**, *9*, 472−482.
(44) Zhang, X.; Wu, X.; Chen, Y.; Zhu, C. Metal-free radical-mediated alkylfunctionalization of ethylene and low-boiling-point alkenes. *Green Chem.* **2023**, *25*, 4234−4238.
(45) Wang, H.; Bellotti, P.; Zhang, X.; Paulisch, T. O.; Glorius, F. A base-controlled switch of SO_2 reincorporation in photocatalyzed radical difunctionalization of alkenes. *Chem.* **2021**, *7*, 3412−3424.
(46) Tan, G.; Das, M.; Keum, H.; Bellotti, P.; Daniliuc, C.; Glorius, F. Photochemical single-step synthesis of β-amino acid derivatives from alkenes and (hetero)arenes. *Nat. Chem.* **2022**, *14*, 1174−1184.
(47) Cai, Y.; Roy, T. K.; Zähringer, T. J. B.; Lansbergen, B.; Kerzig, C.; Ritter, T. Arylthianthrenium salts for triplet energy transfer catalysis. *J. Am. Chem. Soc.* **2024**, *146*, 30474−30482.
(48) Chan, A. Y.; Perry, I. B.; Bissonnette, N. B.; Buksh, B. F.; Edwards, G. A.; Frye, L. I.; Garry, O. L.; Lavagnino, M. N.; Li, B. X.; Liang, Y.; Mao, E.; Millet, A.; Oakley, J. V.; Reed, N. L.; Sakai, H. A.; Seath, C. P.; MacMillan, D. W. C. Metallaphotoredox: The merger of photoredox and transition metal catalysis. *Chem. Rev.* **2022**, *122*, 1485−1542.
(49) Lei, Z.; Wang, C.; Wang, A.; Liu, T.; Dong, Z.; Zhang, W.; Wu, J. Ligand-modulated metal-radical polarity match enables general 1,2-dicarbofunctionalization of ethylene. *Nat. Chem.* **2026**, DOI: 10.1038/s41557-026-02177-8.
(50) Fischer, H.; Radom, L. Factors controlling the addition of carbon-centered radicals to alkenes—an experimental and theoretical perspective. *Angew. Chem., Int. Ed.* **2001**, *40*, 1340−1371.
(51) Nakamura, Y.; Ebeling, B.; Wolpers, A.; Monteil, V.; D'Agosto, F.; Yamago, S. Controlled radical polymerization of ethylene using organotellurium compounds. *Angew. Chem., Int. Ed.* **2018**, *57*, 305−309.
(52) Jin, Y.; Jing, Y.; Li, C.; Li, M.; Wu, W.; Ke, Z.; Jiang, H. Palladium-catalysed selective oxidative amination of olefins with Lewis basic amines. *Nat. Chem.* **2022**, *14*, 1118−1125.
(53) Chen, J.-J.; Zhang, J.-Y.; Fang, J.-H.; Du, X.-Y.; Xia, H.-D.; Cheng, B.; Li, N.; Yu, Z.-L.; Bian, J.-Q.; Wang, F.-L.; Zheng, J.-J.; Liu, W.-L.; Gu, Q.-S.; Li, Z.-L.; Liu, X.-Y. Copper-catalyzed enantioconvergent radical C(sp^3)-N cross-coupling of activated racemic alkyl halides with (hetero)aromatic amines under ambient conditions. *J. Am. Chem. Soc.* **2023**, *145*, 14686−14696.
(54) Hioe, J.; Zipse, H. Radical stability and its role in synthesis and catalysis. *Org. Biomol. Chem.* **2010**, *8*, 3609−3617.
(55) Engl, P. S.; Haring, A. P.; Berger, F.; Berger, G.; Perez-Bitrian, A.; Ritter, T. C-N cross-couplings for site-selective late-stage diversification *via* aryl sulfonium salts. *J. Am. Chem. Soc.* **2019**, *141*, 13346−13351.
(56) Chen, C.; Fu, G. C. Copper-catalyzed enantioconvergent alkylation of oxygen nucleophiles. *Nature* **2023**, *618*, 301−307.
(57) Mao, R.; Frey, A.; Balon, J.; Hu, X. Decarboxylative C(sp^3)-N cross-coupling via synergetic photoredox and copper catalysis. *Nat. Catal.* **2018**, *1*, 120−126.
(58) Liang, Y.; Zhang, X.; MacMillan, D. W. C. Decarboxylative sp^3 C-N coupling via dual copper and photoredox catalysis. *Nature* **2018**, *559*, 83−88.
(59) Cheung, K. P. S.; Fang, J.; Mukherjee, K.; Mihranyan, A.; Gevorgyan, V. Asymmetric intermolecular allylic C-H amination of alkenes with aliphatic amines. *Science* **2022**, *378*, 1207−1213.
(60) Liu, Z.; Li, M.; Deng, G.; Wei, W.; Feng, P.; Zi, Q.; Li, T.; Zhang, H.; Yang, X.; Walsh, P. J. Transition-metal-free C(sp^3)-H/C(sp^3)-H dehydrogenative coupling of saturated heterocycles with N-benzyl imines. *Chem. Sci.* **2020**, *11*, 7619−7625.
(61) Si, X.; Zhang, L.; Wu, Z.; Rudolph, M.; Asiri, A. M.; Hashmi, A. S. K. Visible light-Induced α-C(sp^3)-H acetalization of saturated heterocycles catalyzed by a dimeric gold complex. *Org. Lett.* **2020**, *22*, 5844−5849.
(62) Ding, Y.; Jiang, Y.; Serrat, N. L.; Zhong, K.; Lan, Y.; Ball, Z. T. Copper-mediated cross-coupling selective for pyroglutamate post-translational modifications. *J. Am. Chem. Soc.* **2024**, *146*, 33518−33525.
(63) Yang, T.; Jiang, Y.; Luo, Y.; Lim, J. J. H.; Lan, Y.; Koh, M. J. Chemoselective union of olefins, organohalides, and redox-active esters enables regioselective alkene dialkylation. *J. Am. Chem. Soc.* **2020**, *142*, 21410−21419.
(64) Ye, F.; Zheng, S.; Luo, Y.; Qi, X.; Yuan, W. Ligand-controlled regioreversed 1,2-aryl-aminoalkylation of alkenes enabled by photoredox/nickel catalysis. *ACS Catal.* **2024**, *14*, 8505−8517.
(65) Górski, B.; Barthelemy, A. L.; Douglas, J. J.; Juliá, F.; Leonori, D. Copper-catalysed amination of alkyl iodides enabled by halogen-atom transfer. *Nat. Catal.* **2021**, *4*, 623−630.

https://doi.org/10.1021/jacs.6c03412
J. Am. Chem. Soc. XXXX, XXX, XXX−XXX

(66) Yang, J.; Wang, P.; Neumann, H.; Jackstell, R.; Beller, M. Industrially applied and relevant transformations of 1,3-butadiene using homogeneous catalysts. *Ind. Chem. Mater.* **2023**, *1*, 155−174.
(67) Saleem, M.; Abhishek, P.; Yadagiri, D. Light-induced reactivity of nucleophilic siloxycarbene with heterocumulenes: synthesis of α-ketoamides, hydantoins, oxoacetamidines, and amides. *Org. Lett.* **2024**, *26*, 10291−10298.
(68) Buglioni, L.; Raymenants, F.; Slattery, A.; Zondag, S. D. A.; Noël, T. Technological innovations in photochemistry for organic synthesis: flow chemistry, high-throughput experimentation, scale-up, and photoelectrochemistry. *Chem. Rev.* **2022**, *122*, 2752−2906.
(69) Liu, C. G.; Song, L.; Liu, Q.; Chen, W.; Xu, J.; Wang, M.; Zhang, Y.; Tan, T. W.; Lei, Z.; Cheng, L.; Khan, S. A.; Wu, J. High-speed circulation flow platform facilitating practical large scale heterogeneous photocatalysis. *Org. Process Res. Dev.* **2024**, *28*, 1964−1970.

https://doi.org/10.1021/jacs.6c03412
J. Am. Chem. Soc. XXXX, XXX, XXX−XXX